

RESEARCH

Open Access



# Electronic nose and machine learning for modern meat inspection

Ivan Shtepliuk<sup>1\*</sup>, Guillem Domènech-Gil<sup>1,2</sup>, Viktor Almqvist<sup>3</sup>, Arja Helena Kautto<sup>3</sup>, Ivar Vågsholm<sup>3</sup>, Sofia Boqvist<sup>3</sup>, Jens Eriksson<sup>1</sup> and Donatella Puglisi<sup>1\*</sup>

\*Correspondence:  
ivan.shtepliuk@liu.se; donatella.puglisi@liu.se

<sup>1</sup> Department of Physics, Chemistry and Biology, Linköping University, 581 83 Linköping, Sweden

<sup>2</sup> Department of Thematic Studies and Environmental Change, Linköping University, 581 83 Linköping, Sweden

<sup>3</sup> Department of Animal Biosciences, Swedish University of Agricultural Sciences, 750 09 Uppsala, Sweden

## Abstract

Objective and reliable post-mortem meat inspection is a key factor in ensuring adequate assessment and quality control of meat intended for human consumption. Early identification of issues that may impact public health and animal health and welfare, such as the presence of chemical contaminants in meat, is critical. In this study, we propose a novel method to modernize meat inspection using an electronic nose combined with machine learning (ML), with focus on pig meat as a case study. We explored its potential as a complementary tool to traditional sensory evaluation and analytical methods, aiming to enhance the efficiency and effectiveness of current inspections. We employed a metal-oxide based gas sensor array of commercially available chemoresistive sensors, functioning as an electronic nose, to differentiate between various categories of 100 pig meat samples collected at a slaughterhouse based on their odor characteristics, including a urine-like smell and post-mortem aging. Using the Optimizable Ensemble model, we achieved a sensitivity of 96.5% and specificity of 95.3% in categorizing fresh and urine-contaminated meat samples. The model demonstrated robust predictive performance with a Kappa value of approximately 0.926, indicating near-perfect agreement between the predictions and actual classifications. Furthermore, our developed ML model demonstrated the ability to distinguish between nominally fresh pig meat and meat aged for one to two additional days with an accuracy of 93.5% and can also correctly identify meat aged 3–31 days or 17–31 days. Based on the consensus of preliminary decisions from each individual sensor element, the algorithm effectively determined the final status of the meat. This research lays the groundwork for practical applications within the meat inspection process in slaughterhouses and as quality assurance throughout the meat supply chain. As we continue to refine and validate this method, its potential for real-world implementation becomes increasingly evident.

**Keywords:** Gas sensors, Machine learning, Volatile organic compounds, Odor detection, Meat chain waste, Meat quality assurance, Food safety measures, Chemical contamination, Public health hazards, Animal health and welfare

## Introduction

Chemical contaminants in meat are classified by the European Food Safety Authority as a public health hazard that can impact both human and animal health and welfare [1]. The unpleasant odor of pork, which can arise from various factors such as the

animal's sex, diet, genetics, pre-slaughter stress, living conditions, and storage methods, and is perceived as a combination of sweat, urine, and faeces scents [2], has long been recognized as a significant issue for meat quality. This issue leads to financial losses for both meat producers and sellers [3, 4]. For the former, this means that carcasses with detected organoleptic changes are considered unfit for human consumption and must be disposed of, as required by Article 45 of Commission Implementing Regulation (EU) 2019/627 [5]. Furthermore, the costs associated with pig farming are not recovered and become an economic burden for the entire meat chain, from the primary producer to the processing industry. For the latter, the poor quality of meat, if somehow still on supermarket shelves, disappoints customers, increases distrust in meat sellers, and reduces overall purchases [6]. Reliable and fast tools for increased efficiency and effectiveness of inspections are therefore needed for prevention or early detection of public health hazards such as chemical contamination.

The unpleasant odor, exemplified by boar taint [2], is primarily associated with androstenone [7] and skatole [8]; however, its overall profile is more complex and sensitive to external factors and meat storage time [9–12]. Therefore, the strategy to detect it cannot rely solely on the identification of skatole and androstenone in pig carcasses. It should be consistent across all classes of pigs and adapted for rapid and reliable detection of the odor itself, regardless of the specific volatile compounds (volatolome) that contribute to the smell. This is crucial, as the meat odor profile changes significantly over time [13], influenced by natural hormonal processes, intestinal bacterial metabolism, feed type, race, age, sex status, environment, and meat aging/decomposition. Thus, developing detection methods that capture these dynamic odor profile changes is essential. This strategy would enable fast identification of problematic batches, allowing timely interventions to prevent health hazards and reduce financial losses. Additionally, it would help ensure meat quality, thereby bolstering consumer confidence. Central to this is analyzing the general aroma profile of meat samples and identifying the presence or absence of specific set of volatile organic compounds (VOCs) associated with off-odors using pattern recognition algorithms, rather than detecting individual VOCs as would be done with gas chromatography.

The current methods to evaluate the unpleasant odor, including sensory assessment by trained panels [14], mass spectrometry coupled with gas chromatography (GC–MS) [15–17], surface-enhanced Raman scattering (SERS) [18], enzyme immunoassay (EIA) [19, 20], fluoroimmunoassay (FIA) [21, 22], and colorimetric assay [23] are often time-consuming and expensive, making it difficult to perform rapid, cost-efficient, and objective carcass classification on the slaughter line. Emerging methodologies and new digital technologies have the potential to enable rapid and efficient sample analysis, assessment, and management. One promising approach is the use of a gas sensor array, or electronic nose (*e-nose*), that is an electronic device intended to detect odors. However, *e-noses* themselves are non-specific. Integrating this technology with sophisticated ML models represents a powerful approach to address diverse problems [24–29], particularly in food quality assessment and safety monitoring [30–35]. For instance, Surjith et al. [30] proposed a hybrid model based on an integration of Random Forest (RF), Convolutional Neural Network (CNN), and Gated Recurrent Unit (GRU) that achieved a remarkable accuracy of 99.8% in distinguishing fresh beef from spoiled beef by leveraging data from

*e*-nose sensor composed of 11 elements. Zhan et al. [31] introduced a low-cost colorimetric sensor array based on metal–organic framework (MOF) Fabry–Pérot films, which, when analyzed with standard *k*-nearest neighbour (kNN), demonstrated high classification accuracy (96.7%) for detecting VOCs related to beef spoilage. In a similar vein, Wijaya et al. [32] explored a combination of *e*-nose with 11 sensor elements with filter-based feature selection algorithms and ensemble learning techniques, such as Random Forest and Adaboost, for beef quality assessment. High-performance results of the classification task, including 99.9% accuracy, were achieved. Furthermore, research on the detection of meat adulteration has also advanced. Han et al. [33] developed a low-cost *e*-nose using colorimetric sensors to detect pork adulteration in beef, with the extreme learning machine (ELM) model outperforming traditional methods (91.3% and 87.5% in the training and test sets). Additionally, Huang and Gu [34] introduced a combined one-dimensional convolutional neural network (1DCNN) and a random forest regressor (RFR) framework for quantitative detection of beef adulterated with pork using 10 different MOS sensors as *e*-nose. The coefficient of determination ( $R^2$ ) for this model was estimated to be 99.7%. Similarly, Jia et al. [35] utilized a fusion of near-infrared spectroscopy and *e*-nose data with an F1-score-based model reliability estimation (MRE) method to detect pork adulteration in lamb meat with high accuracy (98.6%). These approaches highlight the effectiveness of combining multiple data sources and ML techniques to improve detection capabilities. These advancements collectively illustrate the growing synergy between *e*-nose technologies and ML methods. The integration of these tools not only enhances the precision and accuracy of meat quality assessment but also provides practical and cost-effective solutions for enhancing food safety measures. Regarding the issue of pork quality, the combination of *e*-nose technology and ML began to be explored in the early 1990s. Research primarily focused on classifying pig meat based on skatole and androstenone levels [36–38]. Annor-Frempong et al. [36] achieved 84.2% accuracy in differentiating boar taint intensities using a 12-conducting-polymer sensor array with a discriminant function algorithm. Their samples were categorized as: (i) normal (skatole < 0.2 µg/g, androstenone < 0.5 µg/g), (ii) doubtful (skatole < 0.2 µg/g, androstenone < 1.0 µg/g), and (iii) abnormal (skatole > 0.2 µg/g, androstenone > 1.0 µg/g). Other studies [37, 38] focused on distinguishing between low and high levels, achieving a classification rate of 85.0%. Despite these advances, effectively discriminating between fresh pork and samples exhibiting urine-like odors remains a challenge that has not yet been thoroughly studied.

The meat industry faces a persistent problem that goes beyond traditional concerns about boar taint: the occurrence of urine-like odors in pig carcasses, including those of castrated males and females. This issue, highlighted by meat producers and confirmed by the Swedish Food Agency, underscores a critical need for innovative detection methods. Assessment of carcass odor is currently performed by official veterinarians and official auxiliaries and is therefore highly subjective. An *e*-nose would provide a more objective sensor-based safety and quality assurance than a subjective organoleptic one. Our study addresses this real-world problem by developing a novel approach that harnesses the power of *e*-nose technology coupled with advanced ML algorithms. Using sensor technology for objective meat inspection is a new research area that offers unprecedented opportunities to modernize official food control. Digital technologies enable

significant improvements in data acquisition, recording, analysis, evaluation, and reporting as well as process automation and remote control. However, the use of new technology, including sensors and artificial intelligence (AI), is currently hindered by various EU regulations (AI-Act, Data Governance Act, Data Act, and General Data Protection Regulation), which limit its application in real-world settings. Compared to other sensor technologies, such as hyperspectral imaging for meat quality evaluation or drones to collect visual data, our proposed solution is potentially cheaper, faster, and easier to implement from a regulatory perspective. Furthermore, *e*-noses allow integration into compact, lightweight, and easy-to-use and maintain devices that do not require specific training, specialized operators, or expensive maintenance. We aim at the creation of a uniform legal framework in the EU to regulate the development, use, and application of sensor- and AI-based new technology, where *e*-noses integrated with AI/ML can be used together with other sensor technologies to modernize meat inspection.

Our goal is to demonstrate a reliable, accurate, and non-invasive method for rapid detection of chemical contaminants in meat. As an initial case study, our objective is to distinguish between fresh pig meat and samples exhibiting urine-like odors, using urine as the chemical contaminant. This approach aims to enhance quality assessment and control measures in meat production, contributing to increase public health, animal health and welfare, and potentially reducing economic losses and improving consumer satisfaction. Furthermore, we extend our methodology to tackle another crucial aspect of meat quality: freshness assessment. By classifying meat samples according to their aging period, ranging from 1 to 31 days, we provide a comprehensive tool for monitoring meat quality. This dual-purpose approach not only addresses the immediate concern of urine odor detection but also offers a broader application in assessing meat freshness, thereby contributing to food safety and quality management in the meat industry. Through this research, we aim to demonstrate the versatility and effectiveness of combining *e*-nose technology with ML in solving complex, real-world challenges in meat production and quality assurance, with focus on pig meat.

## Material and methods

### Sample collection and preparation

We analyzed 100 pig meat samples from Gotland, Sweden, weighing approximately 1.5 g each. Samples were aseptically taken from the diaphragm of pigs slaughtered the day before the start of measurements and shipped in refrigerated bags to preserve freshness. All pigs belonged to the same breed and were housed and managed under the same conditions in intensive production systems. They were slaughtered when they reached a weight of approximately 100 kg. This uniformity in breed, age, and management practices helps ensure that potential variations in results are not due to these factors. The use of samples with known information about their origin, slaughter conditions, and freshness was essential to validate the accuracy and reliability of our proposed method. The delivered samples were stored in a refrigerator at  $+5\text{ }^{\circ}\text{C} \pm 1\text{ }^{\circ}\text{C}$  to ensure their preservation and freshness, and to inhibit bacterial proliferation. The investigation was conducted on samples from both castrated males and intact females aged 6 months within the designated pig population. Meat samples were sent in standard tubes, each capable of holding a maximum of 15 ml. Fifty samples were sent fresh, and other 50 samples

were sent immersed in urine. The urine used for marinating was taken directly from the pig's bladder at the time of slaughter. Each meat sample was marinated in the urine of the same pig from which the meat was taken, maintaining its biological consistency. The marinating process lasted approximately 24 h before the first measurement (day 1). The 24-h marination period was chosen to allow sufficient time for urine-derived volatile compounds to diffuse and equilibrate within the meat sample. Upon visual inspection, the fresh and "contaminated" samples appeared clearly different in color, demonstrating the marinating effect had taken place (see Supplemental Picture S1). To design our experiments, we followed recommendations received from the Swedish Food Agency. These recommendations included the use of urine-contaminated samples, to simulate chemical contamination in an easy and controllable way, and fresh (uncontaminated) samples, as a control group, for comparison. The 24-h time interval before the first measurement corresponding to shipping time is in line with typical meat processing times in industrial settings, where carcasses might be stored for up to 24 h before further processing or inspection [39] and with protocols used in meat quality and safety studies. For instance, Kebede and Getu [40] employed a 24-h incubation period in their bacteriological quality assessment of raw meat, while Feng et al. [41] evaluated quality parameters within a 24-h window post-treatment. These studies demonstrate that a 24-h period is relevant for observing significant changes in meat samples, whether due to bacterial growth or other quality alterations. In our case, this duration allows for the establishment of a stable urine-related VOC profile, mimicking potential real-world scenarios of chemical contamination during processing and storage. It is important to note that consistently applying this marination time across all samples allows the e-nose to detect characteristic changes induced by urine exposure, regardless of the absolute intensity of the odor. We would like to point out that our study aims to demonstrate the ability of our ML model to discriminate among different classes, classified as "good" or "bad". To this end, our study does not aim to specifically detect androstenone and/or skatole as odor-defining compounds. The reasons for our choice to go beyond the issue of boar taint are multiple: we worked with castrated males and intact females, which cannot be associated with boar taint linked to these two molecules; marination in urine was convenient due to the lack of naturally occurring urine-odor samples, since collecting such samples in a single location and during a limited period of time is statistically difficult, labour-intensive, and subjective; unpleasant odors in pork are not limited to the well-known issue of boar taint associated with androstenone and skatole but can also arise from other factors, such as urine contamination on the carcass. Indeed, urine can be regarded as an ideal non-invasive source of VOCs responsible for unpleasant odors [19, 42]. According to control data from the Swedish Food Agency the most common non-compliant carcass odor is urine-odor. In most cases the carcass has a primary pathological process that makes giving this non-compliance unfit for human consumption. In line with this, our goal was to mimic as closely as possible a real-life scenario of non-compliant carcasses with a urine-like odor.

#### **Experimental procedure and measurement protocol**

We implemented a custom metal-oxide-based 32-element *e*-nose, hosted at Sensor and Actuator Systems (SAS) research division of Linköping University, to measure VOC

emissions from fresh and contaminated meat samples using urine, for a total of 100 samples and 900 measurements. Due to proprietary restrictions imposed by the developer, we cannot provide specific information on the types of sensors incorporated into the device. Each sensor measures the temporal evolution of the voltage in response to the VOCs released from the samples. The voltage changes as various VOCs interact with the sensor material, generating a unique response profile for each sensor. This type of sensor is commonly referred to as a metal-oxide semiconductor (MOS) sensor. To differentiate between fresh and spoiled meat we measured the *e*-nose response to the total VOC emissions from samples belonging to different categories. We then applied pattern recognition algorithms to differentiate between them. Since the *e*-nose responses consistently varied between meat samples of different categories, we can conclude that the chemical composition of the odor differs between these two conditions without the need to identify specific chemicals. Please note that “day 0” used to indicate initial measurements refers to samples measured 24 h after slaughter, corresponding to the delivery time from Gotland to Linköping. Following initial measurements (“day 0”), analogous measurements of all samples were conducted over the next 2 days (“day 1” and “day 2”). Three consecutive measurements were performed for each sample to test experimental settings and repeatability of sensor readings. Subsequent experiments to study the VOC emissions produced by the decomposition process of spoiled meat over a month were carried out only with samples of non-contaminated meat. Since urine decomposes rapidly, soon producing a distinctly pungent odor, we considered further measurements of urine-contaminated meat samples to be scientifically irrelevant given the scope of this research. Output signals were collected from meat samples aged for 3, 10, 17, 24, and 31 days, with a gap of 1 week between each series of measurements. These time points were selected to capture the progression of the *e*-nose signals, which are expected to correlate with changes in the meat’s VOC profile as it transitions from fresh to near spoilage. The selection of these specific time points allows us to track changes in the VOC profile at different stages: early changes (1, 2 days), mid-term changes (3, 10 days) and late changes (17, 24, 31 days). This range of time points enables our model to learn and distinguish between changes due to normal aging/decomposition processes. The aging process was not controlled to create dry-aged meat. Samples were allowed to decompose naturally under constant refrigerated conditions ( $+5\text{ }^{\circ}\text{C} \pm 1\text{ }^{\circ}\text{C}$ ) to simulate real-world scenarios of prolonged storage or forgotten meat products. All samples were measured at an ambient temperature of  $+21\text{ }^{\circ}\text{C} \pm 1\text{ }^{\circ}\text{C}$ . Consistent application of storage, environmental, and measurement conditions to all samples minimized the impact of thermal effects and external factors on the results.

We note that we operated the *e*-nose in blind conditions, which means that the ML algorithm analyzed the samples without prior knowledge of their status. We therefore compared the *e*-nose outputs against the known information provided by the veterinarian at the slaughterhouse, which served as reference method to validate the results.

#### **Data processing, feature extraction and dataset formation**

The raw signals were initially normalized using Z-score approach, followed by smoothing via the Savitzky–Golay filter employing a polynomial order of two. It should be noted that the weight of the samples fluctuated within a narrow range, typically within

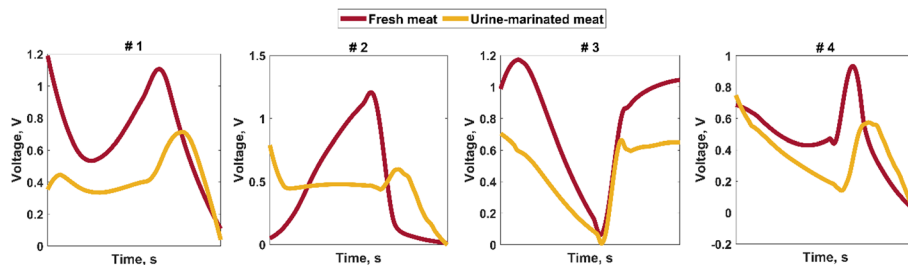
a few tenths of a gram. For the fresh samples, the range from minimum to maximum weight was 0.75 g to 1.82 g (mean  $1.37 \text{ g} \pm 0.25 \text{ g}$ ). Similarly, for the urine-contaminated samples, the range spanned from 0.93 g to 1.78 g (mean  $1.39 \text{ g} \pm 0.27 \text{ g}$ ). To eliminate the influence of variations in sample weight on the sensor readings, the signal was normalized by the sample mass. We extracted 15 features from the raw sensor signals. These features include parameters such as root-mean-square value (RMS), standard deviation (STD), average value (mean), minimum (min), maximum (max), area, shape factor, slope, zero-cross-rate, skewness, kurtosis, range, and Hjorth parameters (activity, mobility, complexity). An additional 15 features were extracted from the smoothed and normalized signals, using the same set of parameters mentioned above. To account for variations in sample weight, each of the 30 features (15 from raw and 15 from smoothed-normalized signals) was normalized by the corresponding sample weight. This normalization step resulted in a total of 60 distinct features. The features were extracted from the data collected by the *e*-nose, which included 32 sensors. Each sensor contributed to the overall dataset, providing the raw signals from which the features were derived. The dataset was divided into training and test sets using MATLAB's *cvpartition* function, which performs stratified random partitioning. This method ensures that both the training set and the test set maintain approximately the same class proportions as the entire dataset. Therefore, the scenario where the test dataset might disproportionately consist of samples from one condition is not possible due to this stratification process. This dataset was then utilized to train a ML model aimed at classifying signals originating from fresh and urine-contaminated meat. The input to the model consisted of the 60 features extracted from the sensor data. The features of each sample were organized into a feature vector, where each vector represented the features of a single sample. The output of the model during training was the classification label for each sample. The samples were categorized into two classes based on their condition: “fresh” or “urine-contaminated”. The model was trained to predict these class labels based on the entered feature vectors. During training, the model learned to associate the input feature vectors with their corresponding class labels. The training process involved adjusting the model parameters to minimize classification errors and improve prediction accuracy. The model's performance was evaluated using the test set to ensure that it could accurately classify new, unseen samples based on the learned features.

### Classifier training and model evaluation

Signal processing, feature extraction, and dataset formation were conducted within the MATLAB environment. The Classification Learner App in MATLAB was subsequently employed to train models for data classification utilizing various supervised ML approaches (classifiers). The performance of each classifier was assessed using the confusion matrix and receiver operating characteristic (ROC) curve. The examination of the confusion matrix, specifically identifying true positives (TP), true negatives (TN), false positives (FP), and false negatives (FN), allowed for the calculation of several crucial performance metrics. These metrics include accuracy, precision, sensitivity, specificity, and the *F*-measure score. After training and validation, the ML model was tested using a separate test dataset to evaluate its performance. Following successful testing, the

**Table 1** Summary of feature descriptions for voltage–time signal analysis

Feature	Meaning	Formula
Root-mean-square	Measure of the effective or average power of the signal	$x_{RMS} = \sqrt{\frac{1}{N} \sum_{n=1}^N  x_n ^2}$
Standard deviation	Measure of the dispersion or spread of the signal values around the mean	$S = \sqrt{\frac{1}{N-1} \sum_{i=1}^N  x_i - \mu ^2}$
Mean	Arithmetic average of the signal values	$\mu = \frac{1}{N} \sum_{i=1}^N x_i$
Minimum	Smallest value observed in the signal	Min(x) function
Maximum	Largest value observed in the signal	Max(x) function
Area	Cumulative sum of the absolute values of the signal over time	Numerical integration via the trapezoidal method
Shape factor	Ratio of the RMS value to the mean value of the signal	$x_{SF} = \frac{x_{RMS}}{\frac{1}{N} \sum_{i=1}^N  x_i }$
Slope	Rate of change of the signal over time	Fit a first-degree polynomial to the data
Zero-crossing rate	Rate at which the signal crosses the zero axis	$ZCR = \frac{1}{2W_L} \sum_{n=1}^{W_L}  sgn[x_i(n)] - sgn[x_i(n-1)] $
Skewness	Measure of the asymmetry of the distribution of signal values	$x_{skew} = \frac{\frac{1}{N} \sum_{i=1}^N  x_i - \bar{x} ^3}{\left[ \frac{1}{N} \sum_{i=1}^N  x_i - \bar{x} ^2 \right]^{3/2}}$
Kurtosis	Measure of the “tailedness” or peakedness of the distribution of signal values	$x_{kurt} = \frac{\frac{1}{N} \sum_{i=1}^N  x_i - \bar{x} ^4}{\left[ \frac{1}{N} \sum_{i=1}^N  x_i - \bar{x} ^2 \right]^2}$
Range	Difference between the maximum and minimum values of the signal	$Range = \max(x) - \min(x)$
Activity	Measure of the overall variance of the signal	$var(x) = \frac{1}{N-1} \sum_{i=1}^N  x_i - \mu ^2$
Mobility	Measure of the rapidity of changes in the signal	$Mobility = \sqrt{\frac{var(\dot{x}(t))}{var(x(t))}}$
Complexity	Measure of the waveform complexity or irregularity of the signal, relative to its mobility	$Complexity = \frac{\sqrt{\frac{var(\ddot{x}(t))}{var(\dot{x}(t))}}}{Mobility}$

**Fig. 1** Comparative analysis of voltage–time curves measured by our e-nose in the presence of fresh and urine-contaminated meat samples. Separate responses from four selected sensing elements of e-nose are shown

trained model was employed for inference, where it was applied to classify additional data beyond the test dataset (Table 1).

## Results and discussion

### Odor profiling: distinguishing fresh from urine-contaminated meat

To begin our investigation, we analyzed the response of selected sensing elements of our e-nose to meat samples with and without marination in urine. Figure 1 illustrates the smoothed and normalized signals from a randomly chosen sample on “day 0”. Our



findings suggest that marination in urine can significantly alter the odor profile of fresh meat samples, as evidenced by distinctive responses across the *e*-nose sensing elements. We observed variations in signal amplitude and shape, potentially indicating urine-related changes in the concentration and composition of emitted VOCs. However, despite these observable differences, our preliminary analysis using principal component analysis (PCA) did not yield clear separation between the two classes (fresh and urine-contaminated meat). This lack of distinct clustering in principle component space indicates that the differences, while present, are not as clear-cut or easy to spot as initially expected. In many cases, the signals from the two classes showed subtle differences, such as small shifts in peak voltage timing or minor amplitude fluctuations. These nuanced variations, while not always resulting in well-separated clusters in principal component space, can be interpreted as meaningful patterns when consistently present. The subtlety of these differences justifies the need for more sophisticated ML techniques to capture and interpret the complex patterns in our data. While Fig. 1 provides an example of sensor signals with noticeable differences between fresh and urine-contaminated pig meat, we could have equally presented signals with minimal visible distinctions. This variability in signal differences underscores the challenge and necessity of advanced ML methods in distinguishing between the “good” and “bad” conditions. These observations create a foundation for developing an ML model capable of distinguishing between the two classes, even when the differences are not immediately apparent through traditional analytical methods. Our approach aims to leverage these subtle but consistent patterns to create a robust classification system for meat freshness and urine contamination detection. This approach should be capable of differentiating samples with varying degrees of urine contamination, including those with low-intensity odor differences. It is important to note that our dataset encompasses a wide range of samples, from those with minimal differences in sensor responses compared to fresh meat, to those with well-perceptible and even strong differences. This variability indicates that the effect of urine marination varies from sample to sample.

We trained all 43 ML models available in MATLAB's Classification Learner. Notably, seven models achieved an accuracy above 91%, underscoring the robustness of our methodology. The consistency across multiple models reinforces the reliability of our approach. The performance of the remaining models was significantly lower, and therefore, they were not mentioned here. For a more detailed overview of their performance, please refer to Supplemental Table S1. Table 2 presents the performance metrics of seven best-performing ML models for classifying meat samples into the fresh or urine-contaminated category. Such a binary information (“fresh” vs. “contaminated”) is sufficient for sanitary inspection and consumer purposes [43].

The models assessed included Narrow Neural Network (NN), Bilayered NN, Medium NN, Wide NN, Optimizable SVM, Optimizable NN, and Optimizable Ensemble. A notable observation is that five out of the seven top-performing models are neural networks, highlighting the effectiveness of this approach for our specific classification task. This predominance of neural network-based models suggests that the complex patterns in our dataset are particularly well-captured by these architectures. Performance metrics such as validation and test accuracies, precision, sensitivity, specificity, and *F*-measure were used to assess the models' effectiveness in classification.

**Table 2** Performance of classifier models for distinguishing “day 0” fresh and urine-contaminated meat samples

Classifier	Validation accuracy, %	Precision, %	Sensitivity,%	Specificity, %	F-measure, %	Test accuracy, %
Narrow NN	91.0	91.1	91.2	91.4	91.1	89.8
Bilayered NN	91.9	92.2	91.2	92.4	91.7	89.9
Medium NN	92.5	92.4	92.3	92.7	92.4	90.8
Wide NN	92.5	92.1	92.5	92.5	92.3	91.9
Optimizable SVM	92.7	92.1	92.9	92.5	92.5	92.2
Optimizable NN	94.2	94.2	93.9	94.4	94.1	94.0
Optimizable Ensemble	95.9	95.1	96.5	95.3	95.8	96.3

It is important to highlight that the results for all models were obtained using a consistent methodological approach. This approach involved utilizing 60 features and implementing a tenfold cross-validation (CV) scheme with a 90%/10% Train/Test Split. Our results demonstrate that the Optimizable Ensemble model outperformed all other models across all performance metrics. The Optimizable Ensemble method used in this study is a ML approach that automatically searches for the best combination of ensemble method (among AdaBoost, RUSBoost, LogitBoost, GentleBoost, and Bag), number of decision tree splits, number of learners, learning rate, and number of predictors to sample, optimizing these hyperparameters within predefined ranges to create a high-performing predictive model. This optimization process results in a high-performing predictive model tailored to the specific characteristics of our data. The core principle underlying the Optimizable Ensemble model hinges on the concept of ensemble learning, wherein a multitude of models undergo independent training, and their interim predictions are combined to formulate a final prediction. The effectiveness of the Optimizable Ensemble model is further exemplified by the specific hyperparameters identified as optimal for our classification task. Through its comprehensive search process, the model converged on a set of parameters that maximized performance for our particular dataset. Specifically, the optimized configuration employed the GentleBoost ensemble method, known for its robustness and ability to handle complex data relationships. This method was coupled with a substantial ensemble of 486 learners, allowing for a diverse and comprehensive model capable of capturing intricate patterns in the data. The learning rate was finely tuned to 0.00115, striking a balance between model convergence and generalization ability. Additionally, the maximum number of splits in the decision trees was set to 27, providing sufficient depth for complex decision boundaries while mitigating overfitting.

In our evaluation, the model demonstrated remarkable proficiency in classifying meat samples, with results that substantiate its effectiveness for this particular application. Specifically, it achieved an impressive accuracy of 95.9% on the validation set, with an even higher test data accuracy of 96.3%, indicating excellent generalization to unseen data. The model's precision of 95.1% underscores its reliability in identifying positive cases, while its high sensitivity of 96.5% showcases its ability to correctly identify a large proportion of fresh meat samples. Moreover, the specificity of 95.3% indicates strong performance in correctly identifying urine-contaminated samples. The *F*-measure of

95.8%, being a harmonic mean of precision and sensitivity, further confirms the model's balanced and robust performance across different aspects of classification. In addition, we calculated the kappa value, diagnostic sensitivity and diagnostic specificity using the test data. The kappa value, a statistical measure assessing agreement between two sets of categorical data [44], demonstrated strong agreement between the model's predictions and actual classifications (Kappa  $\approx$  0.926 that approaches 1 reflecting near-perfect agreement), indicating robust predictive performance. Moreover, the high sensitivity of 97.1% underscores the model's accurate identification of fresh meat samples, while the high specificity of 95.4% highlights its effectiveness in identifying urine-contaminated meat samples. These findings, based on the test data, affirm the model's reliability in real-world scenarios, extending its utility beyond the training phase.

To optimize our model's performance and ensure robust evaluation, we explored various cross-validation and train/test split scenarios. Figure 2 shows the performance comparison of our best model, the Optimizable Ensemble classifier, across these scenarios. The chart clearly illustrates that the tenfold Cross-Validation with 90/10 Train/Test Split (represented by the outer green line) consistently outperforms the other scenarios across all metrics. It yields the highest accuracy in both validation (95.9%) and test (96.3%) phases. This scenario demonstrated the most balanced and impressive performance, with a test confusion matrix showing 95.9% true positive rate and 97.6% true negative rate. The chart's symmetry and outward expansion for this scenario indicate balanced and superior performance across all evaluated aspects.

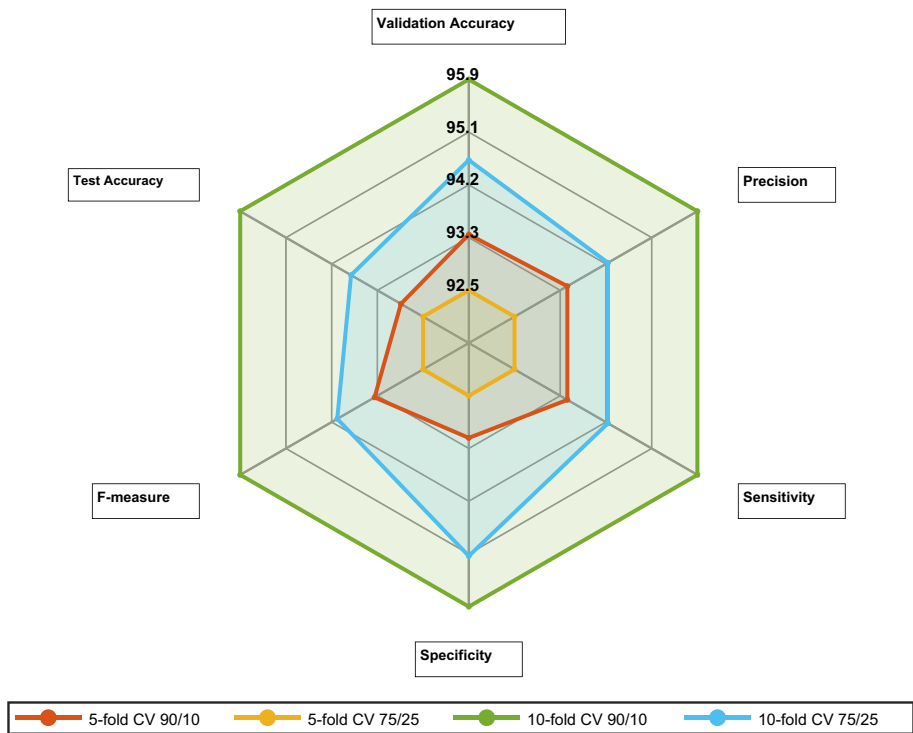


**Fig. 2** A spider chart comparing the performance metrics of four different cross-validation scenarios for the Optimizable Ensemble classifier

The choice of tenfold cross-validation is particularly suitable for our moderate-sized dataset. It strikes an optimal balance between bias and variance, providing more training data per fold compared to fivefold cross-validation, while still maintaining a sufficient number of test samples. The 90%/10% split further maximizes the training data, allowing the model to learn from a broader range of examples without compromising the integrity of the test set.

Notably, this configuration outperformed other scenarios:

- i. Fivefold CV (90%/10%): 93.4% validation accuracy, 93.9% test accuracy
- ii. Fivefold CV (75%/25%): 92.5% validation accuracy, 93.5% test accuracy
- iii. Tenfold CV (75%/25%): 94.6% validation accuracy, 94.8% test accuracy

The tenfold CV with 90%/10% split not only achieved higher accuracies but also demonstrated superior generalization, as evidenced by the closer alignment between validation (95.9%) and test (96.3%) accuracies. This consistency suggests a robust model that is less prone to overfitting, making it ideal for real-world applications in distinguishing between fresh and urine-contaminated meat samples.

In showcasing the excellence of the Optimizable Ensemble classifier, confusion matrices (Fig. 3a, b) and ROC curves (Fig. 3c, d) of the training dataset and of the test dataset were introduced to elucidate its performance. Firstly, the row-normalized

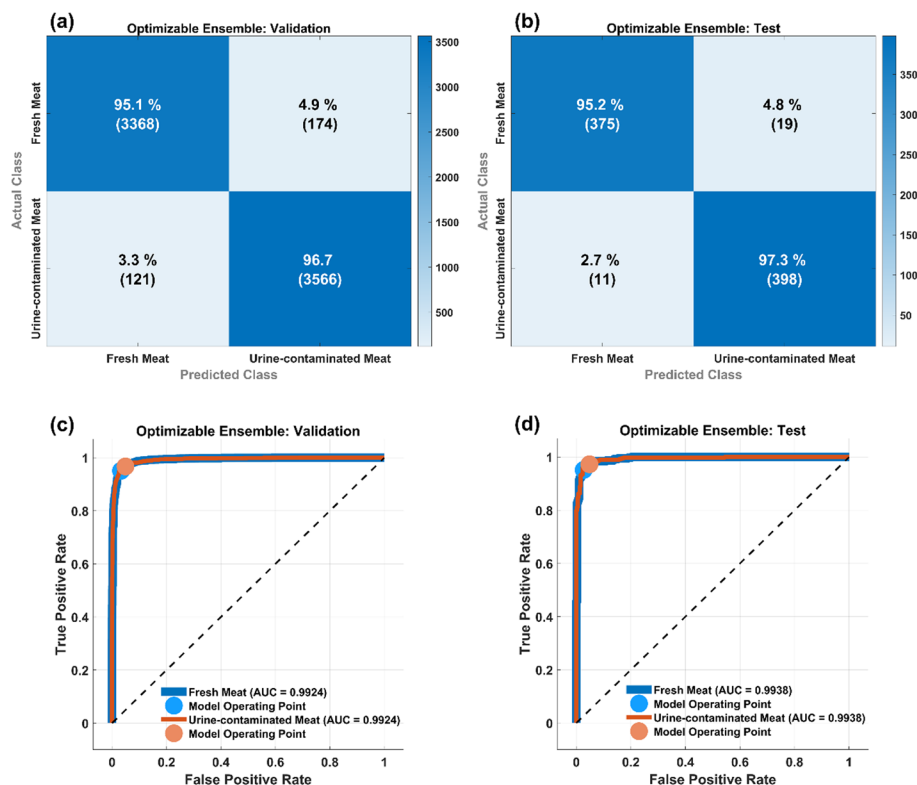


**Fig. 3** Validation and test confusion matrices (a and b) and ROC curves (c and d) for the Optimizable Ensemble classifier, demonstrating its performance in distinguishing “day 0” fresh from urine-contaminated meat samples. For confusion matrices a row normalization was utilized to visualize the percentage of correct predictions for each class

validation (test) confusion matrix provides a comprehensive view of the classifier's effectiveness in distinguishing between classes.

In this representation, the true positives for the “fresh meat” class stand impressively at 95.1% (95.2%), indicating the model's ability to accurately identify fresh meat instances. Meanwhile, the false positives are notably low at 4.9% (4.8%), underscoring the classifier's precision in minimizing misclassifications of urine-contaminated meat as fresh. Although a few instances of fresh meat were erroneously classified as urine-contaminated meat, the false negatives remain relatively low at 3.3% (2.7%), indicating the classifier's robustness in capturing the majority of fresh meat instances. Equally significant is the high true negative percentage of 96.7% (97.3%), highlighting the classifier's proficiency in correctly identifying urine-contaminated meat samples. Secondly, the validation ROC curves provide a graphical representation of the classifier's performance across different discrimination thresholds. The AUC of  $\sim 0.99$  for the ROC curves signifies exceptional discriminatory power, implying that the classifier effectively separates fresh meat from urine-contaminated meat with minimal overlap. The coordinates of the Model Operating Point (MOP) for the current classifier, marked at (0.03, 0.95) for first class and (0.05, 0.97) for second class, reflect a desirable balance between the classifier's performance on both classes. Specifically, the low  $x$ -coordinate indicates the classifier's ability to minimize misclassifications of urine-contaminated meat as fresh, while the high  $y$ -coordinate underscores its efficacy in correctly identifying fresh meat samples. Additionally, the test ROC curves indicates that the model performs very well, further confirming its efficacy in distinguishing between fresh and urine-contaminated meat. In the literature, there is a notable absence of methods specifically developed for discriminating fresh meat from meat intentionally contaminated with urine, as most studies focus on the detection of boar taint. Consequently, it is challenging to make a direct comparison between our model and other existing methods. However, since androstenedione is known to contribute to a urine-like odor, we chose to compare our results with those reported in boar taint detection studies. Comparatively, previous studies in the field of meat classification, such as Annor-Frempong et al. [36], reported an accuracy of 84.2% in differentiating boar taint intensities using a 12-conducting-polymer sensor array coupled with a discriminant function algorithm. Their categorization of samples into normal, doubtful, and abnormal based on skatole and androstenedione concentrations provided a useful but less precise framework for meat classification. Similarly, Bourrounnet et al. [37] and Trout et al. [38] achieved an 85.0% classification rate when distinguishing between low and high levels of boar taint. These earlier studies, although significant in their contributions, demonstrated lower accuracy rates compared to our model, which achieved superior performance in identifying fresh meat. Our model's enhanced accuracy can be attributed to several factors, including a large number of sensors used that generate large datasets, advanced ML algorithms, improved feature selection, and a more refined dataset that likely provided better generalization capabilities.

Next, we developed a user-friendly algorithm for quickly determining the type of meat (Fig. 4) with the final output displayed on the device screen. This algorithm assumes automatic reading of an input file with a *\*.lvm* extension containing raw measurement data of an unknown meat sample (voltage–time curves) for each sensor element, followed by feature extraction. Then, the trained ML model classifies the meat type in

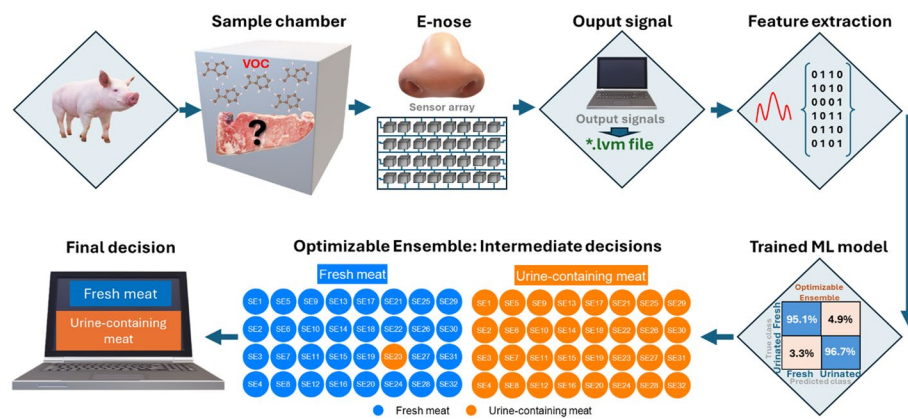


**Fig. 4** Flowchart of the user-friendly algorithm for rapid meat type classification using sensor feedback and majority voting strategy

such a way that intermediate decisions made by each sensor are displayed first, and at the end, a final decision is made based on the majority of intermediate decisions.

This approach helps avoiding the problem where individual sensors may misclassify the meat type. However, since the Optimizable Ensemble classifier already has high accuracy in determining the meat status, we can expect almost unanimous decisions from all sensors, with very rare exceptions. This is precisely illustrated in Fig. 4. Among all sensing elements, only one misclassifies a fresh meat sample as urine-contaminated meat, while the entire set confirms the status of a randomly selected urine-contaminated meat sample.

#### Age identification challenges: electronic nose and machine learning integration

We then pondered: can we accurately identify the age of meat using integrated *e*-nose and ML? To answer this question, we first extracted features from the “day 1” and “day 2” data for both fresh and urine-contaminated meat samples, employing the same procedure as previously, and subsequently compiled a new dataset to train the ML model. This timeframe is relatively short to anticipate significant changes in the odor profile of the meat. However, considering that the meat spoilage process is inevitable and complex (involving the time evolution of bacterial proliferation, microflora, yeast, and mold), it would be reasonable to expect an increase in the concentration of some volatile spoilage markers of pork, such as selected alcohols and aldehydes, even by the second day of meat storage, as demonstrated in the case of atmosphere-packaged minced raw pork [45]. Nevertheless, it was found that Optimizable Ensemble classifier, similar to other classifiers, struggles to differentiate between “day 0” meat and “day 1” and “day 2” meat samples in this three-class problem. The accuracy of such predictive models was below 50%. One of the most likely reasons for this is that the concentrations of targeted VOCs are below the detection limit of the sensor elements in the *e*-nose, and therefore, minor changes in the concentration of these substances cannot be detected by default.

Interestingly, merging the data from “day 1” and “day 2” meat samples into a single class named “days 1–2” and simplifying the problem to a binary classification problem is advantageous for fresh meat, but not for urine-contaminated meat. This finding is particularly relevant because distinguishing between fresh meat and meat that is 1 to

2 days old has practical significance in food safety. Many guidelines and regulations focus on this crucial distinction between fresh meat (day 0) and meat that has begun to age (days 1–2), rather than precise aging durations within the first few days. Furthermore, consumers often categorize meat as either “fresh” or “not fresh”, with less emphasis on the specific number of days since processing. This binary classification (fresh vs. slightly aged) proves more robust and practically applicable, especially given the subtle differences between day 1 and day 2 samples. Moreover, if we aim to develop an algorithm based on ML models capable of not only correctly classifying pork samples for the presence or absence of urine-related VOCs but also determining the approximate age of the meat, it is very important to combine data obtained at different times. The updated classifier achieves an accuracy of 93.5%, allowing for a fairly accurate distinction between fresh and non-fresh meat (further discussed below). Similarly, Chen et al. [46] used a 10-element e-nose to classify pork freshness, achieving 89.5% accuracy. Their classification categorized samples stored for 1–2 days as fresh, 3–4 days as sub-fresh, and 5–7 days as putrid. These results underscore the effectiveness of our model, which outperforms the accuracy reported by Chen et al. in classifying meat freshness.

The ability to differentiate “day 0” fresh meat samples from those aged 1–2 days indicates the potential to expand the initial “day 0” dataset to include “days 0–2” data. The larger and more diverse dataset enhances the model’s robustness, enabling it to perform well on unknown test data. Furthermore, this expansion enables the development of an algorithm based on multiple ML models. The proposed algorithm would first detect the presence or absence of urine-related VOCs and subsequently determine the age of the fresh meat. This was indeed done in the context of this work. Despite the accuracy of the extended model being somewhat reduced compared to its initial counterpart (Fig. 5), the expansion of the dataset from “day 0” to “day 0–2” allows the model to learn how odor profiles evolve over time, thereby capturing more odor patterns.

Leveraging the enriched dataset and the corresponding trained ML models, we aimed to accurately classify meat samples based on both their type (presence of urine or not) and age (Fig. 6). The algorithm started with the collection of data through an e-nose across consecutive days (day 0, day 1, and day 2) for both fresh and urine-contaminated meat samples. Following data acquisition, a robust feature extraction process was conducted to distil relevant information from the raw sensor data. This step aimed to

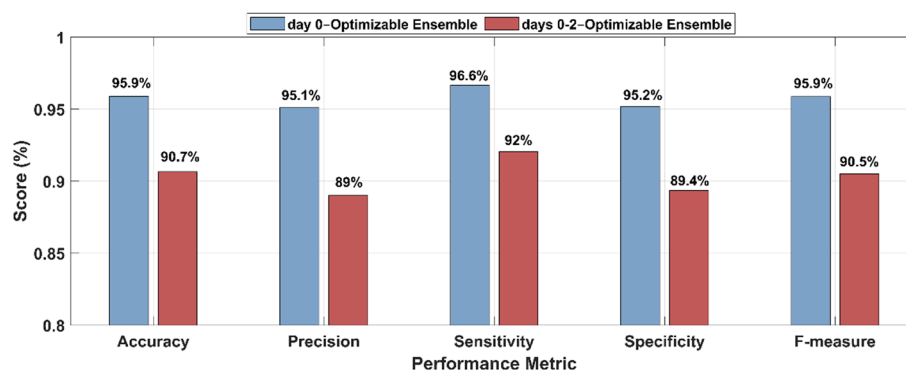


**Fig. 5** Comparison of performance metrics between two models, “day 0”-Optimizable Ensemble and “day 0–2”-Optimizable Ensemble



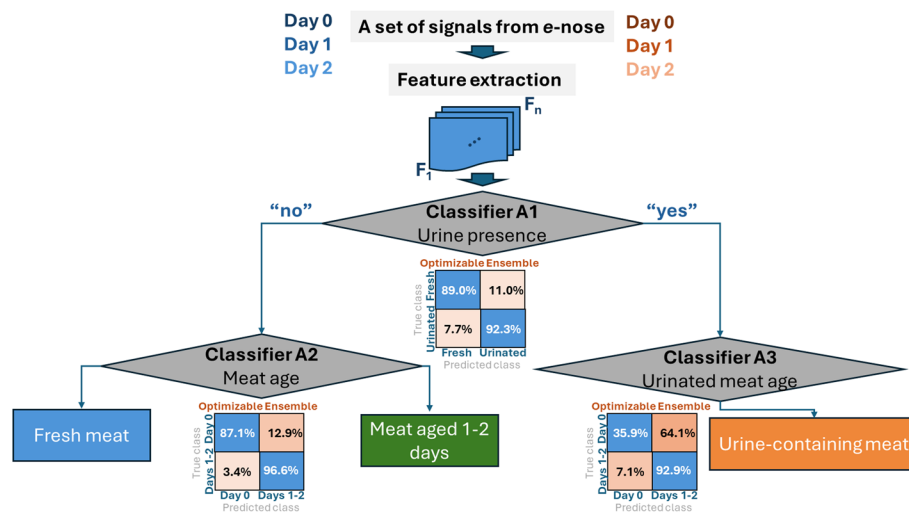


**Fig. 6** Flowchart illustrating the algorithm for classifying meat samples based on type (presence of urine or not) and age, utilizing a combination of data collection, feature extraction, and ML classifiers (**Classifier A1**, **Classifier A2**, and **Classifier A3**)

extract discriminative features that could effectively characterize the VOCs emitted from meat samples, thus enabling accurate classification. Subsequently, a ML model, leveraging the Optimizable Ensemble technique, was trained. This model, designated as **Classifier A1**, was engineered to discern the presence or absence of urine based on the extracted features. Upon evaluation, if **Classifier A1** yielded a negative inference, indicating the absence of urine, the analysis progressed to **Classifier A2**. **Classifier A2**, tailored exclusively on the dataset encompassing “day 0” to “day 1–2” untreated meat samples, was specifically designed to discern the age of the meat. It distinguished between fresh meat samples (day 0) and meat aged for 1 to 2 days (days 1–2), thereby facilitating precise categorization. Conversely, if **Classifier A1** ascertained the presence of urine, the analytical pathway deviated towards **Classifier A3**. Although **Classifier A3** was trained to ascertain the age of urine-contaminated meat samples, it was deemed necessary to streamline the decision-making process, due to its unsatisfactory accuracy. Consequently, the final determination was confined to discerning the status of the meat—whether it was urine-contaminated or not.

As meat ages, it undergoes decay, leading to a noticeable rise in the levels of alcohols and aldehydes, as well as the release of ketones-related VOCs [45]. This makes it more likely to accurately identify the aging status of meat, although it is important to note that the identification will be more about defining a general time frame rather than pinpointing an exact day. In line with this objective, as outlined in “[Material and methods](#)” section, we allowed fresh meat samples to naturally decay over the course of a month. In light of this, an additional approach was developed for determining the age of meat, involving the use of three classifiers (Fig. 7). Initially, all data were divided into two groups: fresh meat (day 0) and non-fresh meat (days 1–31). **Classifier B1** makes the initial decision regarding the freshness of the meat. The ML model behind **Classifier B1** achieved an overall accuracy of 85.7% at the signal level, with a strong ability to correctly identify non-fresh meat



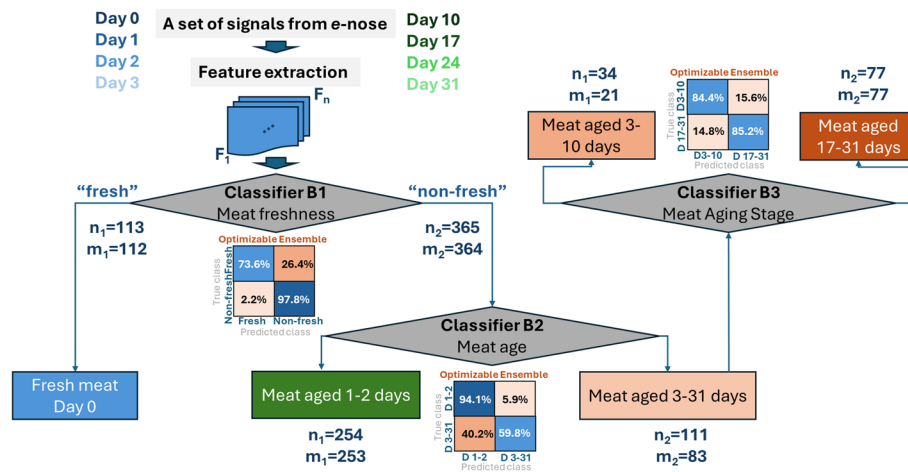


**Fig. 7** Flowchart illustrating the algorithm for classifying meat freshness and aging based on a multi-class approach using three classifiers (**Classifier B1**, **Classifier B2**, and **Classifier B3**). The algorithm categorizes meat samples into distinct aging stages: early aging, mid-aging, and advanced decomposition, facilitating rapid and real-time determination of meat freshness. Note that  $n_{1,2}$  represents the total number of samples in each class being analyzed, while  $m_{1,2}$  denotes the number of correctly classified samples for each class

(97.8% accuracy). After applying the majority voting algorithm at the sample level, **Classifier B1** correctly identified 112 out of 113 fresh samples and 364 out of 365 non-fresh samples. If the sample was classified as fresh, the algorithm concluded with this decision. Otherwise, if the sample was deemed non-fresh, the process continued to **Classifier B2**. **Classifier B2** determined whether the sample belonged to Class 1 (meat aged 1–2 days) or Class 2 (meat aged 3–31 days). At the signal level, the ML model behind **Classifier B2** achieved 94.1% accuracy in identifying 1–2-day-old meat but had a lower accuracy of 59.8% for 3–31-day-old meat, leading to misclassification of some fresher samples as older (40.2%). At the sample level, after majority voting, **Classifier B2** correctly classified 253 out of 254 samples for 1–2-day-old meat, and 83 out of 111 samples for 3–31-day-old meat. If the sample was classified as belonging to Class 1, the process ended with this decision. However, if the sample was assigned to Class 2, the classification process proceeded to **Classifier B3**.

**Classifier B3** refined the aging classification by distinguishing between 3–10 days and 17–31 days. At the sample level, the ML model behind **Classifier B3** struggled with meat aged 3–10 days, correctly classifying only 21 out of 34 samples. However, it showed 100% accuracy (77 out of 77 samples) in identifying meat aged 17–31 days. Of course, such a grouping is somewhat arbitrary, and other options are also possible, like a greater number of classes. However, our choice was based on reflecting three distinct categories of meat aging: (i) early aging, (ii) mid-aging, and (iii) advanced decomposition. The model accurately classify meat aged 17–31 days in 85.2% of cases and meat aged 3–10 days in 84.4% of cases, despite presenting some difficulties in separating the two categories. Although the accuracy of the last two classifiers is lower than the first classifier, we nevertheless consider them to offer reasonably reliable classification. This is mainly due to the fact that all final and intermediate decisions are made based on the majority of intermediate decisions. Consequently, this model has the potential to be used for rapid and real-time determination of meat

age as an indicator of the meat freshness. While the typical refrigerated shelf life of meat is 5–7 days, our study extended well beyond this to explore the full trajectory of meat aging and decomposition. The investigation extended to 17–31 days, while going beyond typical consumption times, offers valuable insights into advanced stages of meat degradation and broadens understanding of the complexity of odor detection and analysis.

## Conclusions

We integrated a metal-oxide gas sensor-based *e*-nose with Optimizable Ensemble ML models, utilizing a rich set of 60 features, to classify pig meat samples with different odor profiles. The *e*-nose's high sensitivity to VOCs, combined with the high predictive capability of the developed ML models and consensus-based decision algorithms, enabled not only a precise classification of urine-contaminated meat with validation accuracy of 95.9% and test accuracy of 96.3%, but also accurate determination of its freshness level. The model demonstrated the ability to distinguish between fresh pig meat and meat aged for 1 to 2 days with an accuracy of 93.5%, and to identify meat aged 3–31 days and 17–31 days. The results presented show the beneficial use of digital technologies to modernize the agritech sector and pave the way for the development of new, rapid, and reliable methods to enhance inspections, slaughter line efficiency, and health and safety measures demonstrating proof of concept at technology readiness level (TRL) 4. It is worth thinking about the settings and context in which our approach should be used. In terms of screening, standardized protocols and procedures should be available to distinguish between true and false positives, while for qualitative information and identification of suspected cases we believe that the presented method is already useful for reaching evidence-based decisions. Our study fits into ongoing international research on modernizing meat inspection and quality control, although the current EU legislation does not allow new technology including AI/ML and sensor technology to replace the official control personnel. Our system is currently intended for research and not to be implemented on an industrial scale for which it would require substantial development, large investments, and corporate management. Before being used on an industrial level, further validation and testing are necessary, in the laboratory as well as in slaughterhouses and food factories. We foresee that sensor-based technology integrated with AI/ML will allow for more affordable, accurate, and reliable safety and quality assurance.

In conclusion, we believe that with adequate calibration, testing, validation, and careful consideration of all experimental conditions the developed system and proposed methodological approach could be extended to other meat industries, contributing to the development of more objective and automated quality assessment methods.

## Abbreviations

ML	Machine learning
GC–MS	Mass spectrometry coupled with gas chromatography
VOCs	Volatile organic compounds
ROC	Receiver operating characteristic
AUC	Area under curve
CV	Cross-validation
NN	Neural network
MOP	Model operating point
MOS	Metal-oxide semiconductor

## Supplementary Information

The online version contains supplementary material available at <https://doi.org/10.1186/s40537-025-01151-4>.

Supplementary Material 1.

Supplementary Material 2.

### Acknowledgements

The authors would like to thank Sagar Ravishankar Maleyur and Lingyin Meng for their invaluable help with the measurements.

### Author contributions

I.S. developed the methodology, performed the investigation, software implementation, data analysis, prepared the visualizations and wrote the original draft. V.A., J.E., G.D.-G., I.V., A.H.K., S.B., and D.P. conceptualized the study. J.E., G.D.-G., and D.P. contributed to methodology development and validation. D.P. supervised the project and managed its administration. J.E., A.H.K., S.B., and D.P. acquired funding for the research. All authors reviewed and edited the manuscript.

### Funding

Open access funding provided by Linköping University. This work was supported by the Swedish Food Agency, Dnr 2021/00918, Vetenskapsrådet (VR), grant No. 2023-07219, VINNOVA Strategic Innovation Program, grant No. 2022-03464, and the European Union's Horizon 2020 research and innovation programme under grant agreement No 101015825. The computations and data handling were enabled by resources provided by the National Academic Infrastructure for Supercomputing in Sweden (NAISS), partially funded by the Swedish Research Council through grant agreement no. 2022-06725.

### Availability of data and materials

The data supporting the findings of this study are available from the corresponding authors upon reasonable request.

## Declarations

### Ethics approval and consent to participate

Not applicable.

### Consent for publication

The authors give the Publisher permission to publish the work.

### Competing interests

The authors declare no competing interests.

Received: 20 November 2024 Accepted: 6 April 2025

Published online: 18 April 2025

## References

- Meat inspection. <https://www.efsa.europa.eu/en/topics/topic/meat-inspection>. Accessed 7 Feb 2025.
- Lundström K, Matthews KR, Haugen J-E. Pig meat quality from entire males. *Animal*. 2009;3(11):1497–507. <https://doi.org/10.1017/S1751731109990693>.
- Kress K, Verhaagh M. The economic impact of German pig carcass pricing systems and risk scenarios for boar taint on the profitability of pork production with immunocastrates and boars. *Agriculture*. 2019;9:204. <https://doi.org/10.3390/agriculture9090204>.
- Karwowska M, Łaba S, Szczepański K. Food loss and waste in meat sector—why the consumption stage generates the most losses? *Sustainability*. 2021;13:6227. <https://doi.org/10.3390/su13116227>.
- Commission Implementing Regulation (EU); 2019. [http://data.europa.eu/eli/reg\\_impl/2019/627/oj](http://data.europa.eu/eli/reg_impl/2019/627/oj). Accessed 27 May 2024.
- Grunert KG. Future trends and consumer lifestyles with regard to meat consumption. *Meat Sci*. 2006;74(1):149–60. <https://doi.org/10.1016/j.meatsci.2006.04.016>.
- Brooks RI, Pearson AM. Steroid hormone pathways in the pig, with special emphasis on boar odour: a review. *J Anim Sci*. 1986;62:632–45. <https://doi.org/10.2527/jas1986.623632x>.
- Claus R, Raab S. Influences on skatole formation from tryptophan in the pig colon. In: Huether G, Kochen W, Simat TJ, Steinhart H, editors. *Tryptophan, serotonin, and melatonin*. Springer; 1999. p. 87–99. [https://doi.org/10.1007/978-1-4615-4709-9\\_87](https://doi.org/10.1007/978-1-4615-4709-9_87).
- Zamaratskaia G, Squires EJ. Biochemical, nutritional and genetic effects on boar taint in entire male pigs. *Animal*. 2009;3(11):1508–21. <https://doi.org/10.1017/S1751731108003674>.
- Andresen Ø. Boar taint related compounds: androstenone/skatole/other substances. *Acta Vet Scand*. 2006. <https://doi.org/10.1186/1751-0147-48-S1-S5>.
- Burgeon C, Debliquy M, Lahem D, Rodriguez J, Ly A, Fauconnier M-L. Past, present, and future trends in boar taint detection. *Trends Food Sci Technol*. 2021;112:283–97. <https://doi.org/10.1016/j.tifs.2021.04.007>.

12. Botelho-Fontela S, Ferreira S, Paixão G, Pereira-Pinto R, Vaz-Velho M, Pires MDA, Silva JA. Seasonal variations on testicular morphology, boar taint, and meat quality traits in traditional outdoor pig farming. *Animals*. 2024;14:102. <https://doi.org/10.3390/ani14010102>.
13. Bleicher J, Ebner EE, Bak KH. Formation and analysis of volatile and odour compounds in meat—a review. *Molecules*. 2022;27:6703. <https://doi.org/10.3390/molecules27196703>.
14. Garrido MD, Egea M, Linares MB, Martínez B, Viera C, Rubio B, Borrisser-Paró F. A procedure for sensory detection of androstenone in meat and meat products from entire male pigs: development of a panel training. *Meat Sci*. 2016;122:60–7. <https://doi.org/10.1016/j.meatsci.2016.07.019>.
15. Burgeon C, Markey A, Debliquy M, Lahem D, Rodriguez J, Ly A, Fauconnier M-L. Comprehensive SPME-GC-MS analysis of VOC profiles obtained following high-temperature heating of pork back fat with varying boar taint intensities. *Foods*. 2021;10(6):1311. <https://doi.org/10.3390/foods10061311>.
16. Font-i-Furnols M, Martín-Bernal R, Aluwé M, Bonneau M, Haugen J-E, Mörlin D, Škrlep M. Feasibility of on/at line methods to determine boar taint and boar taint compounds: an overview. *Animals*. 2020;10(10):1886. <https://doi.org/10.3390/ani10101886>.
17. Wauters J, Vanden Bussche J, Verplanken K, Bekaert KM, Aluwé M, Van den Broeke A, Vanhaecke L. Development of a quantitative method for the simultaneous analysis of the boar taint compounds androstenone, skatole and indole in porcine serum and plasma by means of ultra-high performance liquid chromatography coupled to high resolution mass spectrometry. *Food Chem*. 2015;187:120–9. <https://doi.org/10.1016/j.foodchem.2015.04.066>.
18. Sørensen KM, Westley C, Goodacre R, Engelsen SB. Simultaneous quantification of the boar-taint compounds skatole and androstenone by surface-enhanced Raman scattering (SERS) and multivariate data analysis. *Anal Bioanal Chem*. 2021. <https://doi.org/10.1007/s00216-015-8945-2>.
19. Kumar V, Umapathy G. Development of an enzyme immunoassay to measure urinary and faecal 5 $\alpha$ -androsterone-3-one in pigs. *MethodsX*. 2023;10: 102178. <https://doi.org/10.1016/j.mex.2023.102178>.
20. Leivo J, Mäkelä J, Rosenberg J, Lamminmäki U. Development of recombinant antibody-based enzyme-linked immunosorbent assay (ELISA) for the detection of skatole. *Anal Biochem*. 2016;492:27–9. <https://doi.org/10.1016/j.ab.2015.09.014>.
21. Aguilar-Caballeros MP, Härmä H, Tuomola M, Lövgren T, Gómez-Hens A. Homogeneous stopped-flow fluoroimmunoassay using europium as label. *Anal Chim Acta*. 2002;460(2):271–7. [https://doi.org/10.1016/S0003-2670\(02\)00253-2](https://doi.org/10.1016/S0003-2670(02)00253-2).
22. Tuomola M, Harpio R, Knuuttila P, Mikola H, Lövgren T. Time-resolved fluoroimmunoassay for the measurement of androstenone in porcine serum and fat samples. *J Agric Food Chem*. 1997;45(9):3529–34. <https://doi.org/10.1021/jf9702398>.
23. Fazarinc G, Batorek-Lukač N, Škrlep M, Poklukar K, Van den Broeke A, Kress K, Čandek-Potokar M. Male reproductive organ weight: Criteria for detection of androstenone-positive carcasses in immunocastrated and entire male pigs. *Animals*. 2023;13:2042. <https://doi.org/10.3390/ani13122042>.
24. Ye Y, Liu Y, Li Q. Recent progress in smart electronic nose technologies enabled with machine learning methods. *Sensors*. 2021;21(22):7620. <https://doi.org/10.3390/s21227620>.
25. Domènech-Gil G, Puglisi D. A virtual electronic nose for the efficient classification and quantification of volatile organic compounds. *Sensors*. 2022;22(19):7340. <https://doi.org/10.3390/s22197340>.
26. Domènech-Gil G, Duc NT, Wikner JJ, Eriksson J, Pålédal SN, Puglisi D, et al. Electronic nose for improved environmental methane monitoring. *Environ Sci Technol*. 2024;58(1):352–61. <https://doi.org/10.1021/acs.est.3c06945>.
27. Eriksson J, Puglisi D, Borgfeldt C. Electronic nose for early diagnosis of ovarian cancer. *Proceedings*. 2024;97(1):145. <https://doi.org/10.3390/proceedings2024097145>.
28. Bastos ML, Benevides CA, Zanchettin C, et al. Breaking barriers in *Candida* spp. detection with electronic noses and artificial intelligence. *Sci Rep*. 2024;14:956. <https://doi.org/10.1038/s41598-023-50332-9>.
29. Anwar H, Anwar T, Murtaza S. Review on food quality assessment using machine learning and electronic nose system. *Biosens Bioelectron*. X. 2023;14: 100365. <https://doi.org/10.1016/j.biosx.2023.100365>.
30. Surjith S, Gayathri R, Alex Raj SM. Integrated RF-CNN-GRU ensemble for enhanced beef quality classification: a multi-modal approach. *J Food Compos Anal*. 2024;134: 106503. <https://doi.org/10.1016/j.jfca.2024.106503>.
31. Zhan K, Jiang Y, Qin P, Chen Y, Heinke L. A colorimetric label-free sensor array of metal–organic-framework-based Fabry-Pérot films for detecting volatile organic compounds and food spoilage. *Adv Mater Interfaces*. 2023;10:2300329. <https://doi.org/10.1002/admi.202300329>.
32. Wijaya DR, Afianti F, Arifianto A, Rahmawati D, Kodogiannis VS. Ensemble machine learning approach for electronic nose signal processing. *Sens Bio-Sens Res*. 2022;36: 100495. <https://doi.org/10.1016/j.sbsr.2022.100495>.
33. Han F, Huang X, Aheto JH, Zhang D, Feng F. Detection of beef adulterated with pork using a low-cost electronic nose based on colorimetric sensors. *Foods*. 2020;9(2):193. <https://doi.org/10.3390/foods9020193>.
34. Huang C, Gu Y. A machine learning method for the quantitative detection of adulterated meat using a MOS-based e-nose. *Foods*. 2022;11(4):602. <https://doi.org/10.3390/foods11040602>.
35. Jia W, Qin Y, Zhao C. Rapid detection of adulterated lamb meat using near infrared and electronic nose: A F1-score-MRE data fusion approach. *Food Chem*. 2024;439: 138123. <https://doi.org/10.1016/j.foodchem.2023.138123>.
36. Annor-Frempong E, Nute GR, Wood JD, Whittington FW, West A. The measurement of the responses to different odour intensities of 'boar taint' using a sensory panel and an electronic nose. *Meat Sci*. 1998;50(2):139–51. [https://doi.org/10.1016/S0309-1740\(98\)00001-1](https://doi.org/10.1016/S0309-1740(98)00001-1).
37. Bourrounnet B, Talou T, Gaset A. Application of a multi-gas-sensor device in the meat industry for boar-taint detection. *Sens Actuators B*. 1995;26–27:250–4. [https://doi.org/10.1016/0925-4005\(94\)01596-A](https://doi.org/10.1016/0925-4005(94)01596-A).
38. Trout GR, Salvatore L, McCauley I. Use of an electronic nose to determine boar taint level in pork fat: the effect of relative humidity. In: *Proceedings of the ISOEN 1999*; 1999. p. 321–2.

39. Troy DJ, Kerry JP. Consumer perception and the role of science in the meat industry. *Meat Sci.* 2010;86(1):214–26. <https://doi.org/10.1016/j.meatsci.2009.07.017>.
40. Kebede MT, Getu AA. Assessment of bacteriological quality and safety of raw meat at slaughterhouse and butchers' shop (retail outlets) in Assosa Town, Beneshangul Gumuz Regional State, Western Ethiopia *BMC Microbiol.* 2023;23:403. <https://doi.org/10.1186/s12866-023-03106-2>.
41. Feng X, Jo C, Nam KC, Ahn DU. Impact of electron-beam irradiation on the quality characteristics of raw ground beef. *Innov Food Sci Emerg Technol.* 2019;54:87–92. <https://doi.org/10.1016/j.ifset.2019.03.010>.
42. Jacob CC, Dervilly-Pinel G, Deceuninck Y, Gicquiau A, Chevillon P, Bonneau M, et al. Urinary signature of pig carcasses with boar taint by liquid chromatography-high-resolution mass spectrometry. *Food Addit Contam Part A.* 2017;34(2):218–27. <https://doi.org/10.1080/19440049.2016.1265152>.
43. Wojnowski W, Majchrzak T, Dymerski T, Gębicki J, Namieśnik J. Electronic noses: powerful tools in meat quality assessment. *Meat Sci.* 2017;131:119–31. <https://doi.org/10.1016/j.meatsci.2017.04.240>.
44. Ben-David A. Comparison of classification accuracy using Cohen's Weighted Kappa. *Expert Syst Appl.* 2008;34(2):825–32. <https://doi.org/10.1016/j.eswa.2006.10.022>.
45. Zareian M, Böhner N, Loos HM, Silcock P, Bremer P. Evaluation of volatile organic compound release in modified atmosphere-packaged minced raw pork in relation to shelf-life. *Food Packag Shelf Life.* 2018;18:51–61. <https://doi.org/10.1016/j.fpsl.2018.08.001>.
46. Chen J, Gu J, Zhang R, Mao Y, Tian S. Freshness evaluation of three kinds of meats based on the electronic nose. *Sensors.* 2019;19(3):605. <https://doi.org/10.3390/s19030605>.

## Publisher's Note

Springer Nature remains neutral with regard to jurisdictional claims in published maps and institutional affiliations.